Available online at www.sciencedirect.com
SCIENCE DIRECT®
ELSEVIER
International Journal of Solids and Structures 43 (2006) 27–52
INTERNATIONAL JOURNAL OF SOLIDS and STRUCTURES
www.elsevier.com/locate/ijsolstr

Characterization and modeling of strain assisted diffusion in an epoxy adhesive layer

Samit Roy [a], K. Vengadassalam [a], Yong Wang [a], Soojae Park [b], Kenneth M. Liechti [b,*]

[a] *School of Mechanical and Aerospace Engineering, Oklahoma State University, Stillwater, OK 74078, United States*
[b] *Aerospace Engineering and Engineering Mechanics, University of Texas, Austin, TX 78735, United States*

Received 4 August 2004; received in revised form 2 June 2005
Available online 22 August 2005

Abstract

In this paper a coupled model for strain-assisted diffusion is derived from the basic principles of continuum mechanics and thermodynamics, and material properties characterized using diffusion experiments. The proposed methodology constitutes a significant step toward modeling the synergistic bond degradation mechanism at the bonded interface between a Fiber Reinforced Polymer (FRP) and a substrate, and for predicting debond initiation and propagation along the interface in the presence of a diffusing penetrant at the crack tip and at elevated temperatures. It is now well-known that Fick's law is frequently inadequate for describing moisture diffusion in polymers and polymer composites. Non-Fickian or anomalous diffusion is likely to occur when a polymer is subjected to external stresses and strains, as well as elevated temperatures and humidity. In this paper, a modeling methodology based on the basic principles of continuum mechanics and thermodynamics is developed which allows characterization of the combined effects of temperature, humidity, and strain on diffusion coefficients as well as on moisture saturation level, from moisture weight gain data. For tractability, the diffusion governing equations are simplified for the special case of 1-D diffusion subjected to uniaxial strain and a uniform strain gradient. A novel test specimen that introduces a uniform strain gradient is developed, and diffusion test data for an epoxy-based primer/adhesive are presented and employed for complete characterization of material constants used in the model.

Keywords: Cohesive layer; Characterization; Hygrothermal effect; Non-Fickian diffusion

* Corresponding author. Fax: +1 512 471 5500.
E-mail address: kml@mail.utexas.edu (K.M. Liechti).

0020-7683/$ - see front matter © 2005 Elsevier Ltd. All rights reserved.
doi:10.1016/j.ijsolstr.2005.06.069

1. Introduction

Fiber reinforced polymer (FRP) composites have been extensively used as lightweight, performance-enhancing materials in the aerospace and defense industries. However, FRP is not widely accepted in civil engineering sector primarily due to lack of reliable predictive models and sound design guidelines for their use in civil infrastructure applications. One promising prospect of FRP application in civil engineering is infrastructure repair and retrofit. A major concern for such retrofitting is the debonding of polymeric adhesive that could compromise the reinforcing effect of the FRP. When exposed to harsh environment, degradation of the adhesive bond could lead to delamination of the FRP reinforcement leading to catastrophic failure. Combined exposure to heat and moisture affects a polymer in several ways. The hygrothermal swelling causes a change in the residual stresses within the polymer that could lead to degradation. Further, heat and humidity may cause the matrix to plasticize thus causing an increase in the strain to failure of the polymer. Further, in the event of cyclic heating and cooling with a sustained use-temperature above the boiling point of water, vaporization and out-gassing of absorbed moisture may take place leading to physical damage and chemical changes within the polymer, especially at temperatures higher than glass transition temperature of the polymer matrix. Continuous exposure to high moisture concentrations at the exposed surfaces of the polymer could also initiate damage in the form of polymer cracking, dissolution and peeling.

The processes of sorption in polymeric materials were described in detail by Crank (1975). The influence of moisture diffusion on crack growth along an interface is not yet fully understood. Environmental cracking in a polymer typically occurs in the presence of a penetrant, such as moisture, and stress (or strain). It has been postulated that the mechanism involved in environmental crack growth in a polymer involves a small zone of craze formation and/or plasticization at the crack tip. However, for most thermoset resins such as epoxy, energy absorption at the crack tip is primarily by a shear yielding process and not by crazing. Consequently, for a thermoset epoxy, the zone of plasticization ahead of the crack tip must be determined using a diffusion law for non-porous media, such as Fick's law. However, quite frequently, polymer composites exhibit deviations from the classical Fickian treatment, termed as anomalous or non-Fickian diffusion, especially at elevated temperatures and stress levels, and at high relative humidity. Sophisticated hygrothermal models have been developed and verified by the authors of this paper to account for anomalous diffusion. For stretched polymer sheets where the diffusion-governing equations are coupled with mechanical response through volumetric strain, Roy et al. (1989) presented a numerical procedure for solving coupled strain-assisted diffusion equations using an approach based on free volume theory. Sancaktar and Baechtle (1993) showed that there is a substantial change in the free volume ratio in a polymer as a result of stress whitening, which in turn, results in an increase in moisture uptake in the stress-whitened region. A multi-valued diffusion coefficient, based on an earlier model proposed by Wong and Broutman (1985a,b), was employed to model this effect. More recently, Roy (1999) derived governing equations for history-dependent diffusion using irreversible thermodynamics, and developed a novel numerical framework for solving the complex non-Fickian governing equations using the finite element method.

Stress assisted diffusion in polymers was observed by Fahmy and Hurt (1980) who used a four-point bend specimen to study the effect of bending stress on diffusion in a polymer. They observed that more water uptake occurred on the tensile side than on the compressive side for NARMCO 5208 Epoxy. Subsequently, Weitsman (1987) derived the governing equations for stress-assisted diffusion using principles of continuum thermodynamics. It was reported that both polymer diffusivity and saturation level depend upon stress and that these dependencies can stem from separate aspects of material response, i.e., elastic or viscoelastic material behavior. Sophisticated hygrothermal models have been developed and verified by the authors of this paper to account for various types of anomalous diffusion (Roy et al., 1989, 2000, 2001; Roy, 1999).

The objective of this paper is to predict debond initiation and propagation along a bonded interface in the presence of a diffusing penetrant at the crack tip, and at elevated temperatures. As a step towards

achieving this goal, a coupled model for strain-assisted diffusion is derived from the basic principles of continuum mechanics and thermodynamics that also provide a consistent framework for the derivation of a coupled cohesive-layer constitutive law (Roy and Shiue, 2003). A series of diffusion experiments were conducted to collect moisture weight-gain data in an epoxy specimen under different conditions of temperature, humidity, applied transverse strain, and applied strain gradient. The strain gradient is necessary to accurately simulate the state of strain that typically occurs adjacent to a crack tip along a bonded interface, for example, debond growth in a double cantilever beam subjected to primarily transverse (Mode I) loading. For this purpose, a novel diffusion test specimen was developed for the application of transverse strain as well as a strain gradient during moisture absorption, and this is described in detail in a subsequent section. The effect of viscoelasticity in the cohesive layer on moisture diffusion is not included in the current model in the interest of tractability.

2. Basic equations

2.1. Two-dimensional governing equation

For a two-dimensional cohesive layer of finite thickness h, under plane-strain conditions as shown in Fig. 1, the Helmholtz free energy potential per unit volume is given by,

$$\begin{aligned}\rho\psi = {} & C_0(m,T) + C_1(m,T)\varepsilon_{11} + C_2(m,T)\varepsilon_{22} + C_3(m,T)\varepsilon_{12} + C_4(m,T)\varepsilon_{11}^2 + C_5(m,T)\varepsilon_{22}^2 \\ & + C_6(m,T)\varepsilon_{12}^2 + C_7(m,T)\varepsilon_{11}\varepsilon_{12} + C_8(m,T)\varepsilon_{11}\varepsilon_{22} + C_9(m,T)\varepsilon_{12}\varepsilon_{22} + C_{10}(m,T)\varepsilon_{22}^3 \\ & + C_{11}(m,T)\varepsilon_{22}^2\varepsilon_{12} + C_{12}(m,T)\varepsilon_{22}\varepsilon_{12}^2 + C_{13}(m,T)\varepsilon_{12}^3 + C_{14}(m,T)\varepsilon_{22}^4 + C_{15}(m,T)\varepsilon_{22}^3\varepsilon_{12} \\ & + C_{16}(m,T)\varepsilon_{22}^2\varepsilon_{12}^2 + C_{17}(m,T)\varepsilon_{22}\varepsilon_{12}^3 + C_{18}(m,T)\varepsilon_{12}^4 \end{aligned} \tag{1}$$

where, the mechanical strain components in two-dimensions are defined as,

$$\begin{aligned}\varepsilon_{11} &= E_{11} - \alpha(T - T_{\mathrm{REF}}) - \beta(m - m_{\mathrm{REF}}) \\ \varepsilon_{22} &= E_{22} - \alpha(T - T_{\mathrm{REF}}) - \beta(m - m_{\mathrm{REF}}) \\ \varepsilon_{12} &= E_{12}\end{aligned}$$

and,

ρ mass density of epoxy in the cohesive layer
ε_{11} mechanical strain component in X_1 direction (x-direction)
ε_{22} mechanical strain component normal to crack face in X_2 direction (y-direction)
ε_{12} in-plane shear strain component tangential to crack face

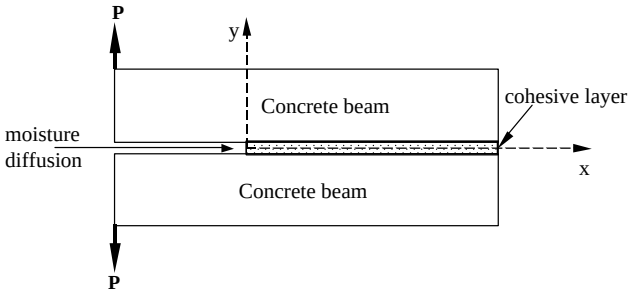

Fig. 1. An epoxy layer with moisture diffusion.

E_{ij} total (kinematic) strain components
m moisture concentration in the cohesive layer at time t
m_{REF} reference moisture concentration
T temperature in the cohesive layer at time t
T_{REF} reference temperature
$\alpha(T)$ isotropic linear coefficient of thermal expansion of polymer
$\beta(T)$ isotropic linear coefficient of moisture expansion of polymer

Chemical potential (μ) of the diffusing vapor in a polymer can be defined as (Weitsman, 1991),

$$\mu = \rho \frac{\partial \psi}{\partial m}$$

or,

$$\mu = \frac{\partial C_0}{\partial m} + \left[\frac{\partial C_4}{\partial m}\varepsilon_{11}^2 - 2C_4(m,T)\beta(T)\varepsilon_{11}\right] + \left[\frac{\partial C_5}{\partial m}\varepsilon_{22}^2 - 2C_5(m,T)\beta(T)\varepsilon_{22}\right] + \left[\frac{\partial C_{10}}{\partial m}\varepsilon_{22}^3 - 3C_{10}(m,T)\beta(T)\varepsilon_{22}^2\right] + \left[\frac{\partial C_{14}}{\partial m}\varepsilon_{22}^4 - 4C_{14}(m,T)\beta(T)\varepsilon_{22}^3\right] \tag{2}$$

It should be noted that in Eq. (2), only dilatational (normal) strains are included because it is assumed that deviatoric (shear) strain does not play a significant role in assisting diffusion. From conservation of mass, the governing Equation for two-dimensional moisture diffusion is,

$$\frac{\partial m}{\partial t} = -\left(\frac{\partial f_x}{\partial x} + \frac{\partial f_y}{\partial y}\right) \tag{3}$$

where the moisture flux, $\vec{f} = f_x\hat{n}_x + f_y\hat{n}_y$, assuming isotropic behavior within the polymer in the absence of temperature gradients is given by,

$$\begin{aligned} f_x &= -\widehat{D}\frac{\partial \mu}{\partial x} \\ f_y &= -\widehat{D}\frac{\partial \mu}{\partial y} \end{aligned} \tag{4}$$

where, $\widehat{D}$ is a material constant. Assuming isotropic material behavior and using the chain rule,

$$\begin{aligned} f_x &= -\widehat{D}\left(\frac{\partial \mu}{\partial m}\right)\frac{\partial m}{\partial x} - \widehat{D}\left(\frac{\partial \mu}{\partial T}\right)\frac{\partial T}{\partial x} - \widehat{D}\left(\frac{\partial \mu}{\partial \varepsilon_{kk}^m}\right)\frac{\partial \varepsilon_{kk}^m}{\partial x} \\ &= -\widehat{D}\left(\frac{\partial \mu}{\partial m}\right)\frac{\partial m}{\partial x} - \widehat{D}\left(\frac{\partial \mu}{\partial T}\right)\frac{\partial T}{\partial x} - \widehat{D}\left(\frac{\partial \mu}{\partial \varepsilon_{11}}\right)\frac{\partial \varepsilon_{11}}{\partial x} - \widehat{D}\left(\frac{\partial \mu}{\partial \varepsilon_{22}}\right)\frac{\partial \varepsilon_{22}}{\partial x} \\ f_y &= -\widehat{D}\left(\frac{\partial \mu}{\partial m}\right)\frac{\partial m}{\partial y} - \widehat{D}\left(\frac{\partial \mu}{\partial T}\right)\frac{\partial T}{\partial y} - \widehat{D}\left(\frac{\partial \mu}{\partial \varepsilon_{11}}\right)\frac{\partial \varepsilon_{11}}{\partial y} - \widehat{D}\left(\frac{\partial \mu}{\partial \varepsilon_{22}}\right)\frac{\partial \varepsilon_{22}}{\partial y} \end{aligned} \tag{5}$$

Assuming isothermal condition and substituting Eq. (5) in Eq. (3), gives

$$\frac{\partial m}{\partial t} = \frac{\partial}{\partial x}\left(D_m\frac{\partial m}{\partial x} + D_{\varepsilon 1}\frac{\partial \varepsilon_{11}}{\partial x} + D_{\varepsilon 2}\frac{\partial \varepsilon_{22}}{\partial x}\right) + \frac{\partial}{\partial y}\left(D_m\frac{\partial m}{\partial y} + D_{\varepsilon 1}\frac{\partial \varepsilon_{11}}{\partial y} + D_{\varepsilon 2}\frac{\partial \varepsilon_{22}}{\partial y}\right) \tag{6}$$

where, the diffusion coefficients are given by,

$$D_m = \widehat{D}\left(\frac{\partial \mu}{\partial m}\right), \quad D_{\varepsilon 1} = \widehat{D}\left(\frac{\partial \mu}{\partial \varepsilon_{11}}\right), \quad D_{\varepsilon 2} = \widehat{D}\left(\frac{\partial \mu}{\partial \varepsilon_{22}}\right)$$

with,

$$D_m = \widehat{D}\left[\frac{\partial^2 C_0}{\partial m^2} + \frac{\partial^2 C_4}{\partial m^2}\varepsilon_{11}^2 - 4\frac{\partial C_4}{\partial m}\beta(T)\varepsilon_{11} + 2C_4(m,T)\beta(T)^2 + \frac{\partial^2 C_5}{\partial m^2}\varepsilon_{22}^2 - 4\frac{\partial C_5}{\partial m}\beta(T)\varepsilon_{22} + 2C_5(m,T)\beta(T)^2 + \frac{\partial^2 C_{10}}{\partial m^2}\varepsilon_{22}^3 - 6\frac{\partial C_{10}}{\partial m}\beta(T)\varepsilon_{22}^2 + 6C_{10}(m,T)\beta(T)^2\varepsilon_{22} + \frac{\partial^2 C_{14}}{\partial m^2}\varepsilon_{22}^4 - 8\frac{\partial C_{14}}{\partial m}\beta(T)\varepsilon_{22}^3 + 12C_{14}(m,T)\beta(T)^2\varepsilon_{22}^2\right] \tag{7a}$$

$$D_{\varepsilon 1} = \widehat{D}\left[2\frac{\partial C_4}{\partial m}\varepsilon_{11} - 2\beta(T)C_4(m,T)\right] \tag{7b}$$

$$D_{\varepsilon 2} = \widehat{D}\left[2\frac{\partial C_5}{\partial m}\varepsilon_{22} - 2\beta(T)C_5(m,T) + 3\frac{\partial C_{10}}{\partial m}\varepsilon_{22}^2 - 6\beta(T)C_{10}(m,T)\varepsilon_{22} + 4\frac{\partial C_{14}}{\partial m}\varepsilon_{22}^3 - 12\beta(T)C_{14}(m,T)\varepsilon_{22}^2\right] \tag{7c}$$

It should be noted that in Eq. (6), the diffusion coefficient D_m is associated with the moisture flux term involving concentration gradient, where as the diffusion coefficients $D_{\varepsilon 1}$ and $D_{\varepsilon 2}$ are associated with flux terms involving strain gradients. From Eq. (7) it is evident that D_m, $D_{\varepsilon 1}$ and $D_{\varepsilon 2}$ are not constants, and they may depend on strain, moisture concentration, and temperature.

2.2. Characterization of boundary condition and saturation concentration

Assuming that the chemical potential of the ambient vapor on the exposed boundary of the cohesive zone remains constant with respect to time (Weitsman, 1991), the resulting concentration at the boundary of the cohesive zone can be derived as,

$$\mu\big(T, m, \varepsilon_{ij}\big)\big|_{\text{BOUNDARY}} = \mu_b(RH, T, \varepsilon_b) \tag{8}$$

where, ε_b is the value of the transverse mechanical strain ε_{22} at the boundary, and RH is the environmental relative humidity. Assuming that in the expression for chemical potential defined in Eq. (2), axial strain $\varepsilon_{11} = 0$, and retaining terms up to second order in ε_{22} (for $\varepsilon_{22} \ll 1$), then Eq. (8) reduces to (Roy and Shiue, 2003),

$$\left\{\widehat{C}_0(\overline{C}_0 + 2\widetilde{C}_0\Delta m) + \frac{27}{8}\frac{\sigma_{\text{MAX}}(T)}{\varepsilon_{\text{MAX}}}\left[(\overline{C}_5 + 2\widetilde{C}_5\Delta m)\varepsilon_{22}^2 - 2\beta(1 + \overline{C}_5\Delta m)\varepsilon_{22}\right] + \frac{27}{2}\frac{\sigma_{\text{MAX}}(T)}{\varepsilon_{\text{MAX}}^2}\left[\beta(1 + \overline{C}_{10}\Delta m)\varepsilon_{22}^2\right]\right\}_{\text{BOUNDARY}} = \mu_b(RH, T, \varepsilon_b) \tag{9}$$

where $\widehat{C}_0, \overline{C}_0, \widetilde{C}_0, \overline{C}_5, \widetilde{C}_5, \overline{C}_{10}$ are material constants independent of temperature and moisture concentration. Substituting for the change in concentration $\Delta m = m_b - m_{\text{REF}}$ in Eq. (9) and solving for m_b gives,

$$m_b = b_0(RH, T) + b_1(RH, T)\varepsilon_b + b_2(RH, T)\varepsilon_b^2 \tag{10}$$

where, m_{REF} is the reference (initial) moisture concentration on the boundary, and b_0, b_1, b_2 are coefficients that depend on relative humidity and temperature, and ε_b is the mechanical strain at the boundary. Therefore, percent weight gain in the epoxy specimen at saturation can be expressed as,

$$M_{\mathrm{MAX}} = \left(\frac{m_b - m_{\mathrm{initial}}}{m_{\mathrm{initial}}}\right) \times (\text{Volume of specimen}) \times 100$$

$$M_{\mathrm{MAX}} = B_0(RH,T) + B_1(RH,T)\varepsilon_b + B_2(RH,T)\varepsilon_b^2 \tag{11}$$

where, B_0, B_1, B_2 are material coefficients that need to be characterized through diffusion experiments.

2.3. Design of experiment

The governing equation for diffusion derived from Helmholtz potential as given by Eq. (6) is a strain-based model. Hence the design of experiment should satisfy the condition that the diffusion is strain assisted rather than stress assisted, in this study. The epoxy material used experiences a large increase in tensile strain due to viscoelastic creep, and so, introduction of constant strain by standard method of loading a specimen by deadweight becomes highly inaccurate. This was the motivation to develop a novel test specimen based on the theory of beam bending that achieves the design of experiment objective and yet remains practical. Further, the test specimen introduces a strain gradient that simulates the decrease in strain along the bond line away from the debond tip subjected to transverse (Mode I) loading.

The experiment is designed with two objectives: (a) being able to introduce a pre-determined strain and strain gradient without any change in applied strain due to viscoelastic creep, and, (b) being able to measure the sample in a laboratory accuracy-balance without much loss of weight gain measurement sensitivity. For this purpose a simple but novel methodology is developed. The epoxy primer is molded onto a flat aluminum strip substrate of thickness 0.51 mm, which is then uniformly bent to calculated radius of curvature to introduce a pre-determined average mid-plane strain as well as strain gradient in the primer as depicted in Fig. 2(a) and (b). An epoxy based primer commercially available under the trade name Waco Mbrace primer is used for this study. The primer is mixed with the hardener and degassed in a degassing chamber to remove any air bubbles present. The surface of the aluminum is etched to ensure proper adhesion between the aluminum and primer. Then the primer layer is molded onto the aluminum substrate in the shape of a 25.4 mm × 25.4 mm coupon, with an average thickness of 0.74 mm. Then these specimens are allowed to cure at room temperature for 72 h and strains are introduced by bending the specimens to the required radius, which is calculated as defined in the following paragraph. These specimens are then pre-conditioned in an electric oven at 93.3 °C for 36 h for drying and for post-curing. After recording the dry weight, the specimens are put in an environmental chamber under various conditions of relative humidity and temperature as listed in Table 3. Knowing the weight of the aluminum strip substrate, the weight of the primer alone can be calculated and the weight-gain due to moisture can be calculated using Eq. (33). A schematic diagram of the specimens used for strain assisted diffusion test is shown in Fig. 2(a) and a photograph of the actual specimen is shown in Fig. 2(b).

As the modulus of aluminum substrate is much greater than that of the epoxy primer, when the aluminum substrate is bent, we can assume that the aluminum and primer are still in linear elastic state and the bonded primer have little effect on the curvature of the aluminum substrate or on the composite beam of aluminum and epoxy primer. Therefore, Kirchhoff's hypothesis of "plane sections remain plane" is valid in this case.

From the force equilibrium on the beam cross section, the x coordinate of the neutral line for the composite beam is given as,

$$x_0 = \frac{E_2 h_2 (h_1 + h_2)}{2E_1 h_1 + 2E_2 h_2} = \frac{h_1 + h_2}{2\left(1 + \frac{E_1 h_1}{E_2 h_2}\right)} \tag{12}$$

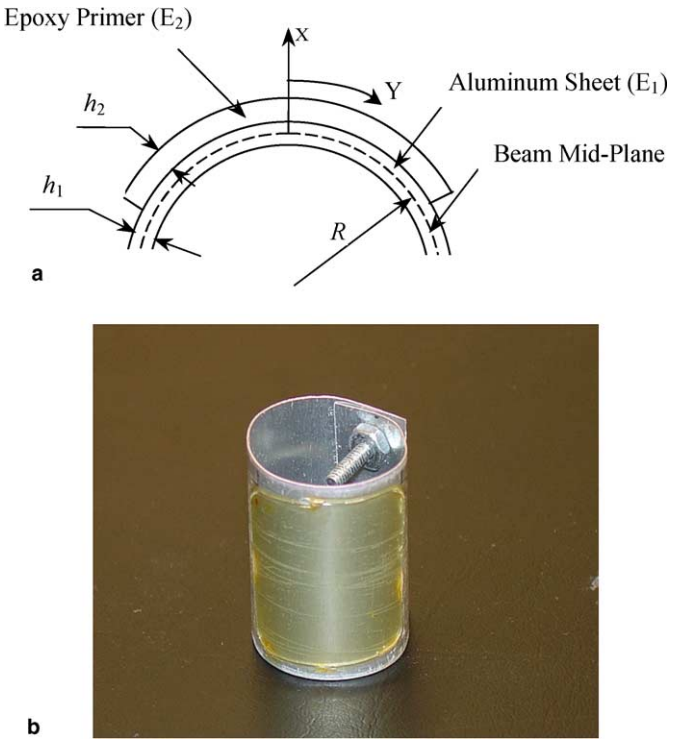

Fig. 2. (a) Schematic diagram of test specimen. (b) Photograph of diffusion specimen showing hollow aluminum cylinder used as substrate.

where,

h_1 – Thickness of aluminum sheet
h_2 – Thickness of epoxy primer
E_1 – Young's modulus of aluminum sheet
E_2 – Young's modulus of epoxy primer
R – Radius of curvature

The total longitudinal strain at the inner surface of the primer is given by, Gere and Timoshenko (1984),

$$\varepsilon_{\text{in}} = \frac{\frac{1}{2}h_1 - x_0}{R + x_0} \tag{13}$$

Strain at the outer surface,

$$\varepsilon_{\text{out}} = \frac{\frac{1}{2}h_1 + h_2 - x_0}{R + x_0} \tag{14}$$

Then the average tensile strain at the mid-plane of the primer is,

$$\varepsilon_{\text{avg}} = \frac{h_1 + \frac{1}{2}h_2 - x_0}{R + x_0} \tag{15}$$

To obtain a specified average total tensile strain ε_{avg} in primer, the radius of the cylinder needs to be

$$R = \frac{h_1 + \frac{1}{2}h_2 - x_0}{\varepsilon_{avg}} - x_0 \tag{16}$$

The Young's modulus of aluminum sheet $E_1 = 75$ GPa, thickness $h_1 = 0.51$ mm and for epoxy primer, $E_2 = 3.85$ GPa, $h_2 = 0.74$ mm, were used in the present study. For the specimen with prescribed 5% average mechanical strain, the radius of curvature is calculated to be $R = 16.69$ mm and for 10% average mechanical strain, the radius is calculated to be $R = 8.35$ mm. Strain gauge test were carried out to calibrate the radius of the specimen to get the required strain.

2.4. Effect of temperature on the radius of the ring specimen

The resulting change in radius of curvature of the aluminum ring due to thermal expansion needs to be evaluated, since the primer specimen is molded onto the flat aluminum strip at room temperature, and the specimen ring as a whole is subjected to elevated temperatures during testing. Linear expansion of the aluminum strip by itself is calculated to study its effect on the specimen as a whole. The specimen is fabricated at room temperature (T_{REF}) of 25.5 °C and then kept in an environmental chamber at temperatures (T) of 32.2 °C (90 F), 40.5 °C (105 F) and 48.9 °C (120 F) for the diffusion tests. The change in length of aluminum ring due to the change in temperature is given by,

$$\Delta l = l_0 \alpha_{Al} \Delta T$$

where

l_0 = Initial circumference length at room temperature
α_{Al} = Coefficient of linear expansion for aluminum (23×10^{-6}/°C)
ΔT = Difference in temperature ($T - T_{REF}$)

For a 10% strain specimen at 48.9 °C the original radius is 8.35 mm, so the initial circumferential length l_0 is 52.46 mm. Therefore the change in length at 48.9 °C is given as 0.03 mm. The final circumference length is given as $l = 52.46 + 0.03 = 52.49$ mm. The radius of the ring after thermal expansion is given as,

$$r = \frac{l}{2\pi}$$

which is calculated to be 8.354 mm. Therefore, the change in ring radius is only 0.048% for the highest test temperature (worst case scenario), which can be neglected without adversely affecting the accuracy of the calculation of strain in epoxy.

2.5. Calculation of mechanical strain in the primer

In the formulation of Helmholtz free energy in Eq. (1), the strain parameters involved are mechanical strains whereas the strains calculated in Eqs. (13)–(15) are total (kinematic) strains. The relationship between total strain and mechanical strain is,

$$\varepsilon_{Mechanical} = \varepsilon_{Total} - \varepsilon_{Hygral} - \varepsilon_{Thermal} \tag{17}$$

where,

$$\varepsilon_{Hygral} = \beta \Delta m$$
$$\varepsilon_{Thermal} = \alpha \Delta T$$

Notice that the relationship between hygral strain and moisture concentration is assumed to be linear even though in some cases, especially for composites, a slight nonlinearity has been found to exist (Tsai et al., 2004). From our experiments on epoxy primer, we determined the average value of $\beta = 100.18 \times 10^{-6}$ mm/mm/RH%, and $\alpha = 97 \times 10^{-6}$ mm/mm/°C respectively at room temperature. Variations in these coefficients as functions of temperature are ignored because of the small temperature range over which diffusion tests were conducted. From these data the maximum, minimum and average mechanical strains and the mechanical strain gradients are calculated and tabulated in Tables 1 and 2 respectively. Since the variation of moisture concentration through thickness of the specimen cannot be measured exactly during a test, therefore the known relative humidity (RH) at the specimen boundaries is used in Eq. (17) to compute mechanical strains.

The moisture weight-gain for each of the specimens is recorded with respect to time, until saturation occurs. Tests are carried out under three different temperatures of 32.2 °C, 40.5 °C and 48.9 °C, and three different environmental moisture concentrations of 75% RH, 85% RH, and 95% RH. For each environmental condition (specified temperature and relative humidity), three total strain levels of 0%, 5% and 10% are tested. The corresponding mechanical strain for each case computed using Eq. (17) is listed in Table 1. A total of 27 diffusion tests were performed with each test data point in Figs. 3–11 representing the average

Table 1
Mechanical strain in each specimen at various environmental conditions

Specimen type	Mech. strain location	Relative humidity (%)								
		75			85			95		
		Temperature (°C)			Temperature (°C)			Temperature (°C)		
		32.2	40.5	48.9	32.2	40.5	48.9	32.2	40.5	48.9
		Mechanical strain (%)			Mechanical strain (%)			Mechanical strain (%)		
Flat (radius = ∞)		0	0	0	0	0	0	0	0	0
Cylindrical (radius = 16.69 mm)	ε_{max}	5.15	5.06	4.99	5.05	4.96	4.89	4.95	4.86	4.79
	ε_{min}	0.72	0.63	0.56	0.62	0.53	0.46	0.52	0.43	0.36
	ε_{avg}	4.46	4.37	4.30	4.36	4.27	4.20	4.26	4.17	4.10
Cylindrical (radius = 8.35 mm)	ε_{max}	11.09	11.01	10.94	10.99	10.91	10.84	10.89	10.81	10.74
	ε_{min}	2.23	2.15	2.08	2.14	2.05	1.98	2.04	1.95	1.88
	ε_{avg}	9.72	9.63	9.56	9.62	9.53	9.46	9.52	9.43	9.36

Table 2
Through-thickness strain gradient in the epoxy specimen at various environmental conditions

Specimen type	Relative humidity (%)								
	75			85			95		
	Temperature (°C)			Temperature (°C)			Temperature (°C)		
	32.2	40.5	48.9	32.2	40.5	48.9	32.2	40.5	48.9
	Mechanical strain gradient (%strain/mm)			Mechanical strain gradient (%strain/mm)			Mechanical strain gradient (%strain/mm)		
Flat (radius = ∞)	0	0	0	0	0	0	0	0	0
Cylindrical (radius = 16.69 mm)	5.98	5.98	5.98	5.98	5.98	5.98	5.98	5.98	5.98
Cylindrical (radius = 8.35 mm)	11.97	11.97	11.97	11.97	11.97	11.97	11.97	11.97	11.97

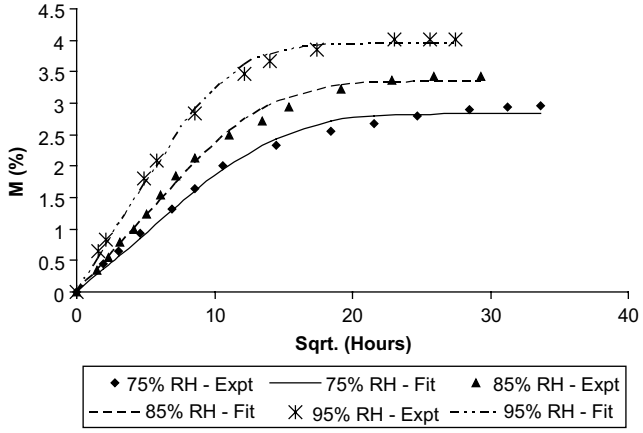

Fig. 3. Moisture uptake vs sqrt. (time) (0% strain, 32.2 °C).

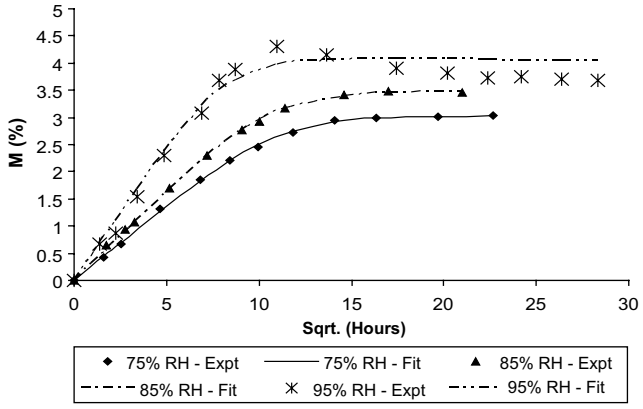

Fig. 4. Moisture uptake vs sqrt. (time) (0% strain, 40.5 °C).

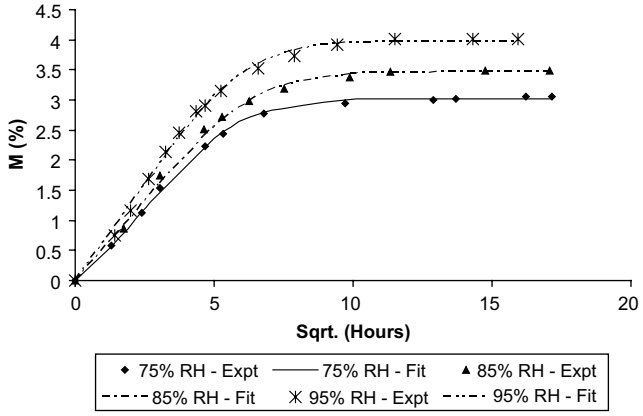

Fig. 5. Moisture uptake vs sqrt. (time) (0% strain, 48.9 °C).

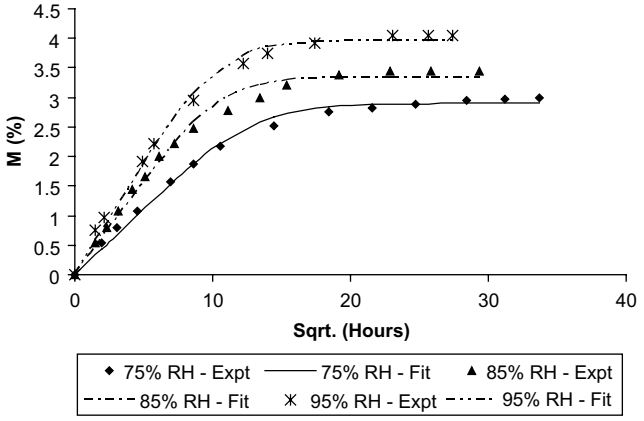

Fig. 6. Moisture uptake vs sqrt. (time) (5% strain, 32.2 °C).

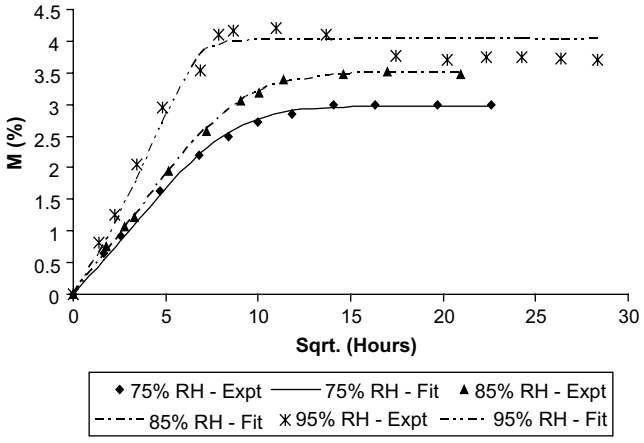

Fig. 7. Moisture uptake vs sqrt. (time) (5% strain, 40.5 °C).

weight-gain from four test specimens. From these test data, diffusion coefficient and saturation moisture concentration could be derived through a nonlinear least-squares technique that is described in the following section.

The bonded electrical resistance strain gage is used to verify that the theoretically computed strain is indeed the strain that is actually introduced in the specimen. A quarter bridge three-wire system with a large strain measurement gage is used. A 10% strain specimen is used to verify the actual strain introduced and thereby to calculate the strain correction factor.

$$\text{Strain correction factor } (\alpha) = \frac{\varepsilon_{\text{actual}}}{\varepsilon_{\text{theory}}}$$

From the strain-gage test the strain correction factor α is found to be 0.87, presumably due to the fact that the ring is not perfectly circular. This correction factor is applied to the calculated radii of all specimens to introduce the correct mid-plane strain.

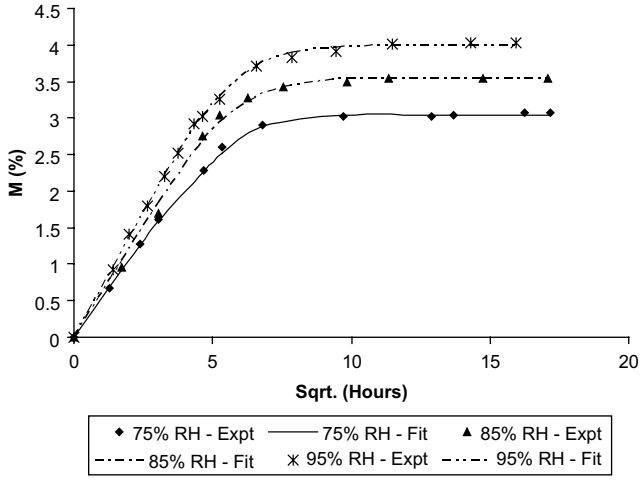

Fig. 8. Moisture uptake vs sqrt. (time) (5% strain, 48.9 °C).

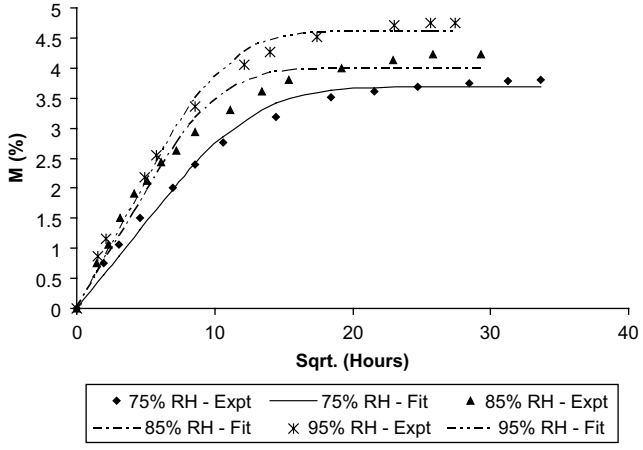

Fig. 9. Moisture uptake vs sqrt. (time) (10% strain, 32.2 °C).

2.6. Calculation of diffusion coefficient and saturation mass uptake

Assuming that moisture diffusion in the thin epoxy layer is primarily through thickness, total moisture uptake based on the one-dimensional form of Fick's law is given by,

$$M(t_k) = M_\infty \left\{ 1 - \frac{8}{\pi^2} \sum_{n=0}^{\infty} \frac{1}{(2n+1)^2} e^{-(2n+1)^2 \left(\frac{\pi}{h}\right)^2 D t_k} \right\} \tag{18}$$

Let

$$E = \sum_{k=1}^{N} [M_k - M(t_k)]^2 \tag{19}$$

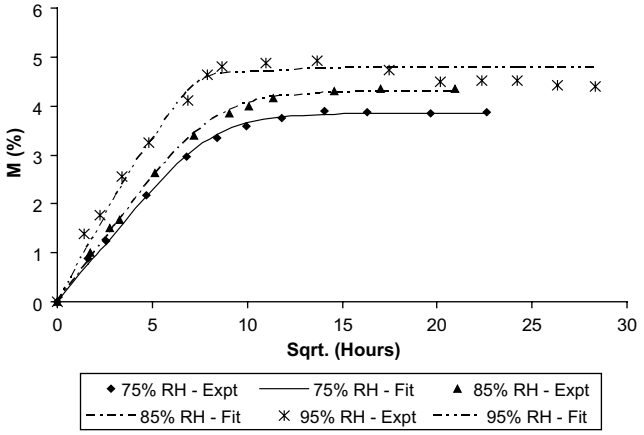

Fig. 10. Moisture uptake vs sqrt. (time) (10% strain, 40.5 °C).

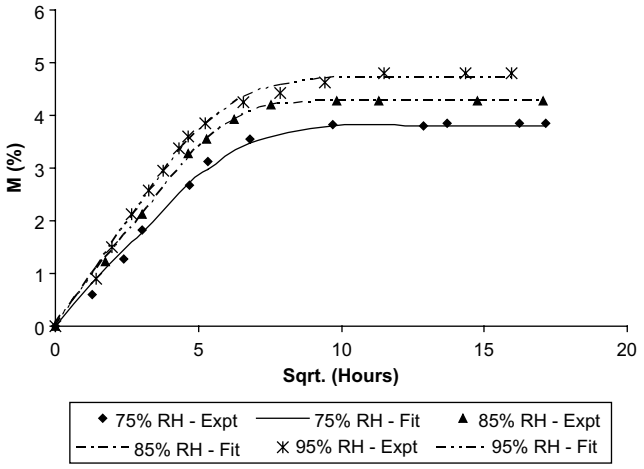

Fig. 11. Moisture uptake vs sqrt. (time) (10% strain, 48.9 °C).

where

E is the least square error
N is the number of test data points
M_k is the kth test data point for mass uptake
t_k is the time corresponding to kth data point during a diffusion experiment
D is the unknown diffusivity
M_∞ is the unknown weight gain % at saturation

For error to be minimum, the first variation of least square error should be zero.

$$\delta E = \sum_{k=1}^{N} -2[M_k - M(t_k)]\delta M(t_k) = 0 \tag{20}$$

But

$$\delta M(t_k) = \frac{\partial M(t_k)}{\partial M_\infty}\delta M_\infty + \frac{\partial M(t_k)}{\partial D}\delta D \tag{21}$$

Substituting Eq. (21) in Eq. (20),

$$\delta E = \left\{\sum_{k=1}^{N}[M_k - M(t_k)]\frac{\partial M(t_k)}{\partial M_\infty}\right\}\delta M_\infty + \left\{\sum_{k=1}^{N}[M_k - M(t_k)]\frac{\partial M(t_k)}{\partial D}\right\}\delta D = 0 \tag{22}$$

Since δM_∞ and δD are arbitrary variations, each of the terms in parenthesis must independently go to zero, that is,

$$\sum_{k=1}^{N}[M_k - M(t_k)]\frac{\partial M(t_k)}{\partial M_\infty} = 0 \tag{23}$$

$$\sum_{k=1}^{N}[M_k - M(t_k)]\frac{\partial M(t_k)}{\partial D} = 0 \tag{24}$$

Expanding Eq. (23)

$$\sum_{k=1}^{N}\left[M_k - M_\infty\left\{1 - \frac{8}{\pi^2}\sum_{n=0}^{\infty}\frac{1}{(2n+1)^2}e^{-(2n+1)^2\left(\frac{\pi}{h}\right)^2 Dt_k}\right\}\right] - \left\{1 - \frac{8}{\pi^2}\sum_{n=0}^{\infty}\frac{1}{(2n+1)^2}e^{-(2n+1)^2\left(\frac{\pi}{h}\right)^2 Dt_k}\right\} = 0$$

$$M_\infty = \frac{\sum_{k=1}^{N}\left[M_k\left\{1 - \frac{8}{\pi^2}\sum_{n=0}^{\infty}\frac{1}{(2n+1)^2}e^{-(2n+1)^2\left(\frac{\pi}{h}\right)^2 Dt_k}\right\}\right]}{\sum_{k=1}^{N}\left[1 - \frac{8}{\pi^2}\sum_{n=0}^{\infty}\frac{1}{(2n+1)^2}e^{-(2n+1)^2\left(\frac{\pi}{h}\right)^2 Dt_k}\right]^2} \tag{25}$$

Expanding Eq. (24),

$$\sum_{k=1}^{N}\left[M_k - M_\infty\left\{1 - \frac{8}{\pi^2}\sum_{n=0}^{\infty}\frac{1}{(2n+1)^2}e^{-(2n+1)^2\left(\frac{\pi}{h}\right)^2 Dt_k}\right\}\right]$$
$$- \left\{(M_\infty)\frac{8}{\pi^2}\sum_{n=0}^{\infty} - \frac{1}{(2n+1)^2}(2n+1)^2\left(\frac{\pi}{h}\right)^2 t_k e^{-(2n+1)^2\left(\frac{\pi}{h}\right)^2 Dt_k}\right\} = 0$$

$$\sum_{k=1}^{N}\left[\begin{array}{l}(M_k)(M_\infty)\frac{8}{\pi^2}t_k\sum_{n=0}^{\infty}\frac{1}{(2n+1)^2}e^{-(2n+1)^2\left(\frac{\pi}{h}\right)^2 Dt_k} - \\ (M_\infty)^2\left\{1 - \frac{8}{\pi^2}\sum_{n=0}^{\infty} - \frac{1}{(2n+1)^2}e^{-(2n+1)^2\left(\frac{\pi}{h}\right)^2 Dt_k}\right\}\left\{\frac{8}{\pi^2}t_k\sum_{n=0}^{\infty}\frac{1}{(2n+1)^2}e^{-(2n+1)^2\left(\frac{\pi}{h}\right)^2 Dt_k}\right\}\end{array}\right] = 0 \tag{26}$$

Substituting Eq. (25) in Eq. (26) results in a highly nonlinear equation in diffusivity (D) that must be solved using iterative procedure. A software code in programming language C was written to solve this numerically. Once diffusivity (D) is obtained from Eq. (26), it can be substituted in Eq. (25) to evaluate weight gain % at saturation (M_∞). The computed diffusivity and saturation mass for all test conditions are listed in Table 3.

Table 3
Diffusivity and M_{max} for different conditions of temperature, relative humidity and strain

Temperature (°C)	Relative humidity (%)	Total strain (%)	Representative specimen	Diffusivity (cm^2/s) $\times 10^{-9}$	M_{max} (%)
32.2	75	0	4	5.8220	2.9486
		5	4	5.9532	2.9848
		10	4	6.2772	3.7839
	85	0	4	7.7720	3.3402
		5	4	8.4432	3.3398
		10	4	10.3720	4.1039
	95	0	4	12.0880	3.9786
		5	4	13.2530	3.9848
		10	4	19.1720	4.7139
40.5	75	0	4	10.1770	3.0302
		5	4	10.4780	3.0219
		10	4	10.6510	3.8484
	85	0	4	12.6470	3.4749
		5	4	13.8740	3.5028
		10	4	16.7710	4.2985
	95	0	4	18.7780	4.0400
		5	4	20.7380	4.0360
		10	4	25.0860	4.7730
48.9	75	0	4	11.5210	3.0150
		5	4	12.0070	3.0457
		10	4	13.1110	3.8064
	85	0	4	17.4410	3.4602
		5	4	19.5980	3.5298
		10	4	24.6970	4.2795
	95	0	4	22.7000	4.0244
		5	4	24.6090	4.0312
		10	4	30.0080	4.7529

2.7. Characterization of nonlinear diffusion coefficients

Revisiting the non-Fickian diffusion governing equation, Eq. (6),

$$\frac{\partial m}{\partial t} = \frac{\partial}{\partial x}\left(D_m \frac{\partial m}{\partial x} + D_{\varepsilon 1}\frac{\partial \varepsilon_{11}}{\partial x} + D_{\varepsilon 2}\frac{\partial \varepsilon_{22}}{\partial x}\right) + \frac{\partial}{\partial y}\left(D_m \frac{\partial m}{\partial y} + D_{\varepsilon 1}\frac{\partial \varepsilon_{11}}{\partial y} + D_{\varepsilon 2}\frac{\partial \varepsilon_{22}}{\partial y}\right) \tag{27}$$

and imposing the condition that the diffusion experiments conducted in this study is a special case of one-dimensional diffusion in the (thickness) x-direction, with an uniform transverse tensile strain in the y-direction having a uniform tensile strain gradient through the thickness (refer to Fig. 2(b)), Eq. (27) reduces to,

$$\frac{\partial m}{\partial t} = \frac{\partial}{\partial x}\left(D_m \frac{\partial m}{\partial x} + D_{\varepsilon 1}\frac{\partial \varepsilon_{11}}{\partial x} + D_{\varepsilon 2}\frac{\partial \varepsilon_{22}}{\partial x}\right) \tag{28}$$

In the absence of applied strain in the x-direction, $\varepsilon_{11} = -v\varepsilon_{22}$, and $\frac{\partial \varepsilon_{11}}{\partial x} = -v\frac{\partial \varepsilon_{22}}{\partial x}$, where v is the Poisson's ratio of the epoxy. Hence, the governing equation for this particular study reduces to,

$$\frac{\partial m}{\partial t} = \frac{\partial}{\partial x}\left(D_m \frac{\partial m}{\partial x} + (D_{\varepsilon 2} - vD_{\varepsilon 1})\frac{\partial \varepsilon_{22}}{\partial x}\right) \tag{29}$$

From the data presented in Table 2 it is evident that the through-thickness gradient of the transverse strain $\left(\frac{\partial \varepsilon_{22}}{\partial x}\right)$ is sufficiently large (up to 12% per mm) that it cannot be ignored. Hence the expected diffusion behavior in the epoxy specimens should be non-Fickian. However, the actual moisture uptake data from diffusion experiments (Refer to Figs. 3–11) indicate that the moisture uptake in the epoxy primer generally obeys Fick's law at least for the range of temperatures, relative humidity, and average strains considered in this study, although the magnitude of the diffusivity and saturation levels for each case depends on the ambient conditions. This observation is based on the fact that the data from diffusion experiments (shown by the symbols) in Figs. 3–11 are in good agreement with the Fickian curve fit (indicated by the dashed lines) for each set of environmental conditions considered in the test matrix. It can therefore be concluded without loss of generality that this particular epoxy material behaves in a concentration-dependent Fickian manner rather than in a strain gradient induced non-Fickian manner. This observation is corroborated by the absorption-desorption curves shown in Fig. 12 for the case of 10% strain, 95% RH, and 48.9 °C, where the desorption curve does not follow the Fickian absorption curve, indicating concentration-dependent diffusion (Crank, 1975). Consequently, the non-Fickian diffusion coefficient ($D_{\varepsilon 2} - vD_{\varepsilon 1}$) in Eq. (29) can be characterized as negligibly small for this material, and the final diffusion governing equation reduces to,

$$\frac{\partial m}{\partial t} = \frac{\partial}{\partial x}\left(D_m \frac{\partial m}{\partial x}\right) \tag{30}$$

which is essentially Fick's law, with a diffusion coefficient D_m that depends on temperature, moisture concentration, and applied strains as defined in Eq. (7a). Since $\beta(T) \ll 1$, we may ignore all the terms beyond first order, while for the transverse strain ε_{22} we retain only up to quadratic term in the expression with $\varepsilon_{11} = -v\varepsilon_{22}$ under uniaxial tension, giving,

$$D_m = \widehat{D}\left[\frac{\partial^2 C_0}{\partial m^2} - v\frac{\partial^2 C_4}{\partial m^2}\varepsilon_{22}^2 + 4v\frac{\partial C_4}{\partial m}\beta(T)\varepsilon_{22} + \frac{\partial^2 C_5}{\partial m^2}\varepsilon_{22}^2 - 4\frac{\partial C_5}{\partial m}\beta(T)\varepsilon_{22} - 6\frac{\partial C_{10}}{\partial m}\beta(T)\varepsilon_{22}^2\right]$$

Re-arranging strain-dependent terms in ascending order, D_m can be expressed as,

$$D_m = \widehat{D}\left[\frac{\partial^2 C_0}{\partial m^2} + \left\{4v\frac{\partial C_4}{\partial m}\beta(T) - 4\frac{\partial C_5}{\partial m}\beta(T)\right\}\varepsilon_{22} + \left\{-v\frac{\partial^2 C_4}{\partial m^2} + \frac{\partial^2 C_5}{\partial m^2} - 6\frac{\partial C_{10}}{\partial m}\beta(T)\right\}\varepsilon_{22}^2\right] \tag{31}$$

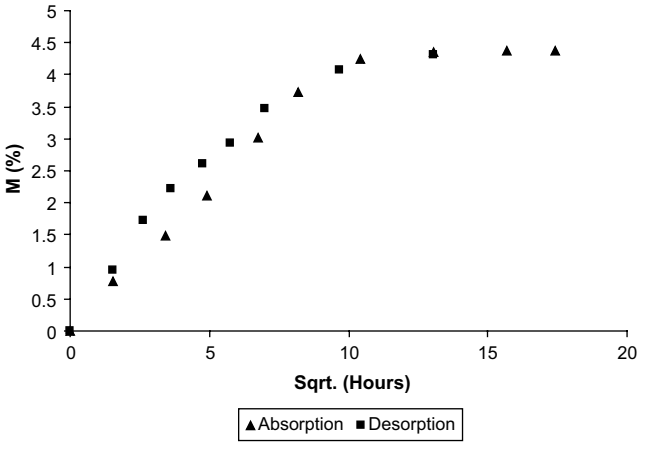

Fig. 12. Moisture absorption–desorption vs sqrt. (time) for epoxy primer (10% strain, 95% RH, 48.9 °C).

Introducing normalized temperature,

$$\overline{T} = \frac{T}{T_{\mathrm{REF}}} \tag{32}$$

where, $T_{\mathrm{REF}} = 40.5\ ^{\circ}\mathrm{C}$, and, following Crank (1975), we define an approximate relationship for the mean value of diffusivity given by,

$$\overline{D}_m = \frac{1}{m_{\max}} \int_0^{m_{\max}} D_m \, \mathrm{d}m \tag{33}$$

where, the maximum concentration is defined as,

$$m_{\max} = \frac{M_{\mathrm{saturation}} - M_{\mathrm{dry}}}{\text{Volume of specimen}}$$

Because there is a significant variation in the mechanical strain through the thickness of the epoxy layer (see Table 1), the average mechanical strain ($\bar{\varepsilon}_{22}$) at the mid-plane of the epoxy layer was used in Eq. (31) to compute diffusivity. Assuming quadratic dependence of diffusivity on temperature and concentration, and using separation of variables Eq. (31) can be written as,

$$\begin{aligned} D_m(m, \overline{T}, \bar{\varepsilon}_{22}) &= F_1(m) F_2(\overline{T}) F_3(\bar{\varepsilon}_{22}) \\ &= (a_{11} + a_{12} m + a_{13} m^2)(a_{21} + a_{22}\overline{T} + a_{23}\overline{T}^2)(a_{31} + a_{32}\bar{\varepsilon}_{22} + a_{33}\bar{\varepsilon}_{22}^2) \end{aligned} \tag{34}$$

Applying the definition of mean value of diffusivity described in Eq. (33) and (34),

$$\overline{D}_m(m_{\max}, \overline{T}, \bar{\varepsilon}_{22}) = \left(a_{11} + \frac{1}{2} a_{12} m_{\max} + \frac{1}{3} a_{13} m_{\max}^2\right)(a_{21} + a_{22}\overline{T} + a_{23}\overline{T}^2)(a_{31} + a_{32}\bar{\varepsilon}_{22} + a_{33}\bar{\varepsilon}_{22}^2)$$

Expanding the above equation, we have,

$$\begin{aligned} \overline{D}_m(m_{\max}, \overline{T}, \bar{\varepsilon}_{22}) &= (D_1 + D_2 m_{\max} + D_3 \overline{T} + D_4 m_{\max}^2 + D_5 \overline{T}^2 + D_6 m_{\max}\overline{T} \\ &\quad + D_7 m_{\max}\overline{T}^2 + D_8 m_{\max}^2 \overline{T} + D_9 m_{\max}^2 \overline{T}^2) \\ &\quad + (D_{10} + D_{11} m_{\max} + D_{12}\overline{T} + D_{13} m_{\max}^2 + D_{14}\overline{T}^2 + D_{15} m_{\max}\hat{T} \\ &\quad + D_{16} m_{\max}\overline{T}^2 + D_{17} m_{\max}^2 \overline{T} + D_{18} m_{\max}^2 \overline{T}^2)\bar{\varepsilon}_{22} \\ &\quad + (D_{19} + D_{20} m_{\max} + D_{21}\overline{T} + D_{22} m_{\max}^2 + D_{23}\overline{T}^2 + D_{24} m_{\max}\overline{T} \\ &\quad + D_{25} m_{\max}\overline{T}^2 + D_{26} m_{\max}^2 \overline{T} + D_{27} m_{\max}^2 \overline{T}^2)\bar{\varepsilon}_{22}^2 \\ \overline{D}_m(m_{\max}, \overline{T}, \bar{\varepsilon}_{22}) &= D_0(m_{\max}, \overline{T}) + D_1(m_{\max}, \overline{T})\bar{\varepsilon}_{22} + D_2(m_{\max}, \overline{T})\bar{\varepsilon}_{22}^2 \end{aligned} \tag{35}$$

where,

$$\begin{aligned} D_0(m_{\max}, \overline{T}) &= D_1 + D_2 m_{\max} + D_3\overline{T} + D_4 m_{\max}^2 + D_5\overline{T}^2 + D_6 m_{\max}\overline{T} + D_7 m_{\max}\overline{T}^2 + D_8 m_{\max}^2\overline{T} \\ &\quad + D_9 m_{\max}^2\overline{T}^2 \\ D_1(m_{\max}, \overline{T}) &= D_{10} + D_{11} m_{\max} + D_{12}\overline{T} + D_{13} m_{\max}^2 + D_{14}\overline{T}^2 + D_{15} m_{\max}\hat{T} + D_{16} m_{\max}\overline{T}^2 \\ &\quad + D_{17} m_{\max}^2\overline{T} + D_{18} m_{\max}^2\overline{T}^2 \\ D_2(m_{\max}, \overline{T}) &= D_{19} + D_{20} m_{\max} + D_{21}\overline{T} + D_{22} m_{\max}^2 + D_{23}\overline{T}^2 + D_{24} m_{\max}\overline{T} + D_{25} m_{\max}\overline{T}^2 \\ &\quad + D_{26} m_{\max}^2\overline{T} + D_{27} m_{\max}^2\overline{T}^2 \end{aligned} \tag{36}$$

There are a total of 27 unknowns which can be computed from the 27 data points for diffusion coefficient listed in Table 3 by means of a least-squares technique as described below. Eq. (35) can be expressed in the following general form,

$$\overline{D}_m(m_{\max}, \overline{T}, \bar{\varepsilon}_{22}) = \sum_{i=1}^{N} D_i f_i(m_{\max}, \overline{T}, \bar{\varepsilon}_{22}) \tag{37}$$

where, N is the number of unknowns ($N = 27$ in this study), D_i are the unknown coefficients, $f_i(k) \equiv f_i(m_{\max_k}, \overline{T}_k, \bar{\varepsilon}_k)$ are the known functions of $m_{\max}, \overline{T},$ and $\bar{\varepsilon}_{22}$. These 27 known functions are defined in Appendix A. From Eq. (37), summation of square error E can be defined as,

$$\begin{aligned} E &= \sum_{k=1}^{M} (\widetilde{D}_k - D(m_{\max k}, \overline{T}_k, \bar{\varepsilon}_k))^2 = \sum_{k=1}^{M} \left[\widetilde{D}_k - \sum_{i=1}^{N} D_i f_i(m_{\max k}, \overline{T}_k, \bar{\varepsilon}_k) \right]^2 \\ &= \sum_{k=1}^{M} \left[\widetilde{D}_k - \sum_{i=1}^{N} D_i f_i(k) \right]^2 \end{aligned} \tag{38}$$

where, M is the total number of test data points ($M = N = 27$ in this study, but in general M and N need not be equal), $f_i(k) \equiv f_i(m_{\max_k}, \overline{T}_k, \bar{\varepsilon}_k)$, $\widetilde{D}_k$ is the value of diffusivity for the kth test data point, D_k is the derived diffusivity from curve fit, and $m_{\max_k}$, $\overline{T}_k$, and $\bar{\varepsilon}_k$ are maximum moisture concentration, normalized temperature, and the average transverse mechanical strain respectively, corresponding to the kth test data point.

To minimize the least squares error,

$$\frac{\partial E}{\partial D_i} = 0 \quad (i = 1, 2, 3, \ldots, N)$$

Therefore,

$$\begin{aligned} &D_1 \sum_{k=1}^{N} f_1(k) f_1(k) + D_2 \sum_{k=1}^{N} f_1(k) f_2(k) + D_3 \sum_{k=1}^{N} f_1(k) f_3(k) + \cdots + D_N \sum_{k=1}^{N} f_1(k) f_N(k) = \sum_{k=1}^{N} \widetilde{D}_k f_1(k) \\ &D_1 \sum_{k=1}^{N} f_2(k) f_1(k) + D_2 \sum_{k=1}^{N} f_2(k) f_2(k) + D_3 \sum_{k=1}^{N} f_2(k) f_3(k) + \cdots + D_N \sum_{k=1}^{N} f_2(k) f_N(k) = \sum_{k=1}^{N} \widetilde{D}_k f_2(k) \\ &\cdots \\ &D_1 \sum_{k=1}^{N} f_N(k) f_1(k) + D_2 \sum_{k=1}^{N} f_N(k) f_2(k) + D_3 \sum_{k=1}^{N} f_N(k) f_3(k) + \cdots + D_N \sum_{k=1}^{N} f_N(k) f_N(k) = \sum_{k=1}^{N} \widetilde{D}_k f_N(k) \end{aligned} \tag{39}$$

The unknown diffusivity coefficients $D_1, D_2, \ldots, D_{27}$ are obtained by solving Eq. (39) simultaneously.

2.8. Characterization of moisture saturation coefficients

Revisiting Eq. (11), and assuming quadratic dependence on temperature and relative humidity, and using separation of variables,

$$\begin{aligned} M_{\mathrm{MAX}}(RH, \overline{T}, \varepsilon_b) &= B_0(RH, \overline{T}) + B_1(RH, \overline{T})\varepsilon_b + B_2(RH, \overline{T})\varepsilon_b^2 = F_1(RH) F_2(\overline{T}) F_3(\varepsilon_b) \\ &= (c_{11} + c_{12} RH + c_{13} RH^2)(c_{21} + c_{22}\overline{T} + c_{23}\overline{T}^2)(c_{31} + c_{32}\varepsilon_b + c_{33}\varepsilon_b^2) \end{aligned} \tag{40}$$

Expanding the above equation, we have,

$$\begin{aligned} M_{\mathrm{MAX}}(RH,\overline{T},\varepsilon_b) = {} & (B_1 + B_2RH + B_3\overline{T} + B_4RH^2 + B_5\overline{T}^2 + B_6RH\overline{T} + B_7RH\overline{T}^2 \\ & + B_8RH^2\overline{T} + B_9RH^2\overline{T}^2) \\ & + (B_{10} + B_{11}RH + B_{12}\overline{T} + B_{13}RH^2 + B_{14}\overline{T}^2 + B_{15}RH\overline{T} + B_{16}RH\overline{T}^2 \\ & + B_{17}RH^2\overline{T} + B_{18}RH^2\overline{T}^2)\varepsilon_b \\ & + (B_{19} + B_{20}RH + B_{21}\overline{T} + B_{22}RH^2 + B_{23}\overline{T}^2 + B_{24}RH\overline{T} + B_{25}RH\overline{T}^2 \\ & + B_{26}RH^2\overline{T} + B_{27}RH^2\overline{T}^2)\varepsilon_b^2 \end{aligned} \tag{41}$$

where,

$$\begin{aligned} B_0(RH,\overline{T}) = {} & B_1 + B_2RH + B_3\overline{T} + B_4RH^2 + B_5\overline{T}^2 + B_6RH\overline{T} + B_7RH\overline{T}^2 \\ & + B_8RH^2\overline{T} + B_9RH^2\overline{T}^2 \\ B_1(RH,\overline{T}) = {} & B_{10} + B_{11}RH + B_{12}\overline{T} + B_{13}RH^2 + B_{14}\overline{T}^2 + B_{15}RH\overline{T} + B_{16}RH\overline{T}^2 \\ & + B_{17}RH^2\overline{T} + B_{18}RH^2\overline{T}^2 \\ B_2(RH,\overline{T}) = {} & B_{19} + B_{20}RH + B_{21}\overline{T} + B_{22}RH^2 + B_{23}\overline{T}^2 + B_{24}RH\overline{T} + B_{25}RH\overline{T}^2 \\ & + B_{26}RH^2\overline{T} + B_{27}RH^2\overline{T}^2 \end{aligned} \tag{42}$$

There are again a total of 27 unknowns which are computed from the 27 test diffusion coefficient data by curve fit technique as described below.

Eq. (41) can be expressed in the following general form,

$$M_{\mathrm{MAX}}(RH,\overline{T},\varepsilon_b) = \sum_{i=1}^{27} B_i f_i(RH,\overline{T},\varepsilon_b) \tag{43}$$

where B_i are the unknown coefficients, $f_i(k) \equiv f_i(RH_k,\overline{T}_k,\varepsilon_k)$ $(i = 1, 2, 3, \ldots, 27)$ are known functions of $RH,\overline{T},\varepsilon_b$, as discussed in the previous section and given in Appendix B.

From Eq. (43), summation of squares of error E can be formed as

$$E = \sum_{k=1}^{N}(M_k - M_{\mathrm{MAX}})^2 = \sum_{k=1}^{N}\left[M_k - \sum_{i=1}^{27} B_i f_i(RH_k,\overline{T}_k,\varepsilon_k)\right]^2 = \sum_{k=1}^{N}[M_k - \sum_{i=1}^{27}\hat{B}_i f_i(k)]^2 \tag{44}$$

where, $N = 27$ is the number of test data points, $f_i(k) \equiv f_i(RH_k,\overline{T}_k,\varepsilon_k)$, M_k the saturation concentration for the kth test data point, and RH_k, $\overline{T}_k$, ε_k and are relative humidity, normalized temperature, and transverse strain on specimen boundary respectively, corresponding to the kth test data point. To minimize the least-squares error,

$$\frac{\partial E}{\partial B_i} = 0 \quad (i = 1, 2, 3, \ldots, 27)$$

Therefore,

$$
\begin{aligned}
&B_1\sum_{k=1}^{N} f_1(k)f_1(k) + B_2\sum_{k=1}^{N} f_1(k)f_2(k) + B_3\sum_{k=1}^{N} f_1(k)f_3(k) + \cdots + B_N\sum_{k=1}^{N} f_1(k)f_N(k) = \sum_{k=1}^{N} M_k f_1(k)\\
&B_1\sum_{k=1}^{N} f_2(k)f_1(k) + B_2\sum_{k=1}^{N} f_2(k)f_2(k) + B_3\sum_{k=1}^{N} f_2(k)f_3(k) + \cdots + B_N\sum_{k=1}^{N} f_2(k)f_N(k) = \sum_{k=1}^{N} M_k f_2(k)\\
&\cdots\\
&B_1\sum_{k=1}^{N} f_N(k)f_1(k) + B_2\sum_{k=1}^{N} f_N(k)f_2(k) + B_3\sum_{k=1}^{N} f_N(k)f_3(k) + \cdots + B_N\sum_{k=1}^{N} f_N(k)f_N(k) = \sum_{k=1}^{N} M_k f_N(k)
\end{aligned}
\tag{45}
$$

The unknown saturation coefficients $B_1, B_2, \ldots, B_{27}$ are obtained by solving Eq. (45) simultaneously.

3. Results and discussions

As presented in Figs. 3–12, the moisture uptake data indicates that the moisture sorption-desoprtion in this material can be characterized as concentration-dependent Fickian diffusion rather than Non-Fickian diffusion. As discussed earlier, the non-linearity can be attributed to the presence of strain and environmental condition of elevated temperature and moisture concentration, and not due to the presence of strain gradient.

The diffusivity and mass saturation for various conditions of temperature, relative humidity, and strain are tabulated in Table 3. As evident from the Table, the influence of temperature, moisture concentration, and strain on diffusivity and maximum saturation concentration is significant. For example, an increase in applied total transverse strain from 0 to 10% results in a 18% increase in m_{sat} and 32% increase in diffusivity (D_m) at 48.9 °C and 95% RH. Interestingly, diffusivity data plotted in Fig. 13 seems to indicate a strong coupling between applied strain and moisture concentration, regardless of test temperature. At lower moisture concentrations (75% RH), the diffusivity data show little or no change with increasing strain; however, they show significant strain dependence at elevated concentrations (85% and 95% RH), thereby validating

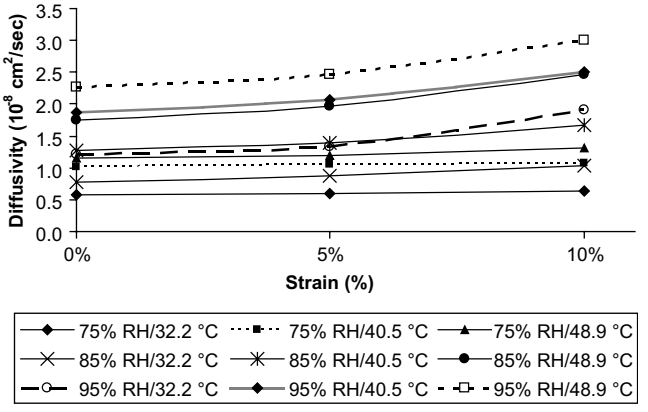

Fig. 13. Influence of total transverse strain on diffusivity.

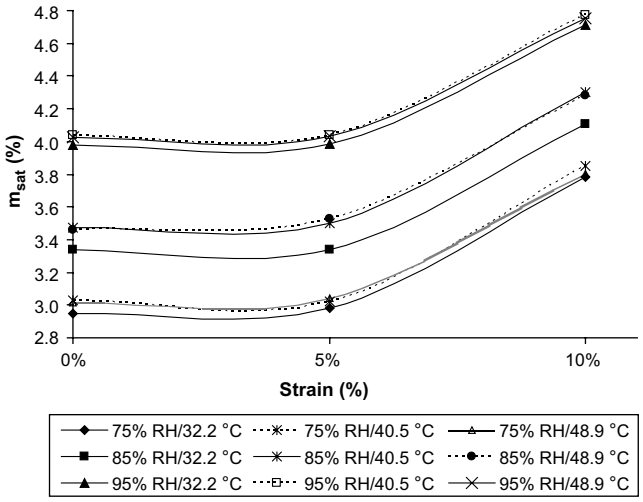

Fig. 14. Influence of total strain on percentage moisture uptake at saturation.

Table 4
Strain-diffusivity coefficients D_0, D_1, D_2

Temp. (°C)	Environmental relative humidity (%)								
	75%			85%			95%		
	D_0	D_1	D_2	D_0	D_1	D_2	D_0	D_1	D_2
32.2	0.582	0.069	3.860	0.777	1.684	9.160	1.209	−2.424	95.080
40.5	1.018	0.730	−2.600	1.265	0.760	33.600	1.878	1.530	47.800
48.9	1.152	0.370	12.200	1.744	1.380	58.800	2.270	0.290	70.200

Table 5
Strain-saturation coefficients B_0, B_1, B_2

Temp. (°C)	Environmental relative humidity (%)								
	75%			85%			95%		
	B_0	B_1	B_2	B_0	B_1	B_2	B_0	B_1	B_2
32.2	2.949	−5.218	114.97	3.340	−5.923	117.12	3.979	−5.397	111.56
40.5	3.030	−6.623	127.65	3.475	−5.262	117.42	4.040	−5.688	115.35
48.9	3.015	−4.936	111.24	3.460	−3.619	103.11	4.024	−5.204	111.62

the coupled diffusion model presented herein at least in a qualitative sense. On the other hand, the tets data for percentage moisture uptake at saturation (M_{max}) plotted in Fig. 14 as a function of strain indicate very little coupling between applied strain and moisture concentration, regardless of test temperature. It is interesting to note that the M_{max} values remain relatively unchanged between 0% and 5% transverse total strain for the entire range of temperature and relative humidity used in the test matrix. While the increase in diffusivity with strain occurs gradually over the entire range of strain at elevated concentrations (Fig. 13), in

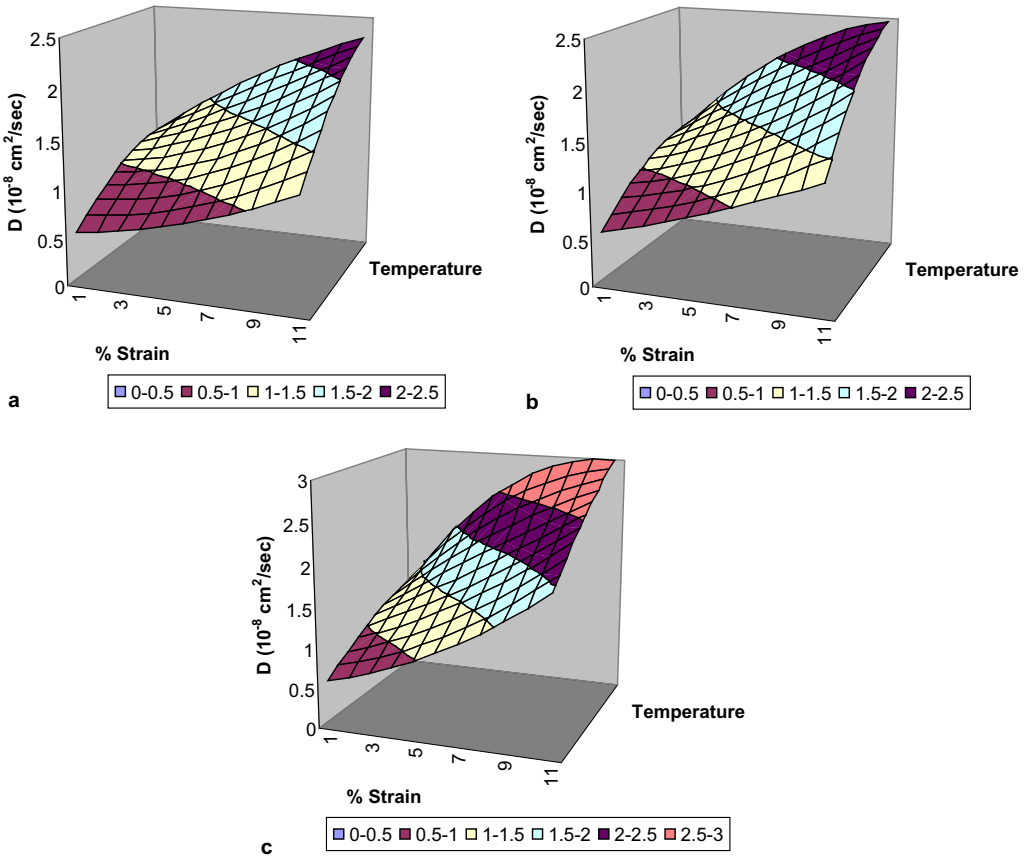

Fig. 15. (a) Diffusivity vs strain and temperature at 75% RH; (b) diffusivity vs strain and temperature at 85% RH; (c) diffusivity vs strain and temperature at 95% RH.

the case of percentage uptake at saturation (M_{max}) the effect of strain becomes evident only for total strains greater than 5% (Fig. 14), indicating a threshold value of strain below which the moisture uptake at saturation is independent of strain for the range of temperatures and relative humidity conditions tested. Test specimens were examined under an optical microscope for evidence of microcracking and/or debonding at 10% strain, but no microcracks or debonds were observed to explain the sudden increase in moisture uptake.

The strain-diffusivity coefficients (D_0, D_1, D_2) and strain-saturation coefficients (B_0, B_1, B_2) are tabulated in Tables 4 and 5 respectively as functions of temperature and relative humidity. As presented in Eq. 11, the mechanical strain value used for calculating B_0, B_1 and B_2 is the mechanical strain at the boundary, i.e., at the top surface of the primer and not the average mechanical strain. Three-dimensional surface plots of the variation of the diffusivity coefficient (D_m) of the epoxy primer with respect to strain and temperature for relative humidity values of 75%, 85% and 95% are given in Fig. 15a, b and c respectively. The variation of percent moisture uptake at saturation (M_{max}) with respect to strain and relative humidity for a temperature value of 32.2 °C, 40.5 °C and 48.9 °C are given in Fig. 16a,b and c respectively. From these plots it is again evident that applied strain has a significant influence over diffusivity and saturation concentration.

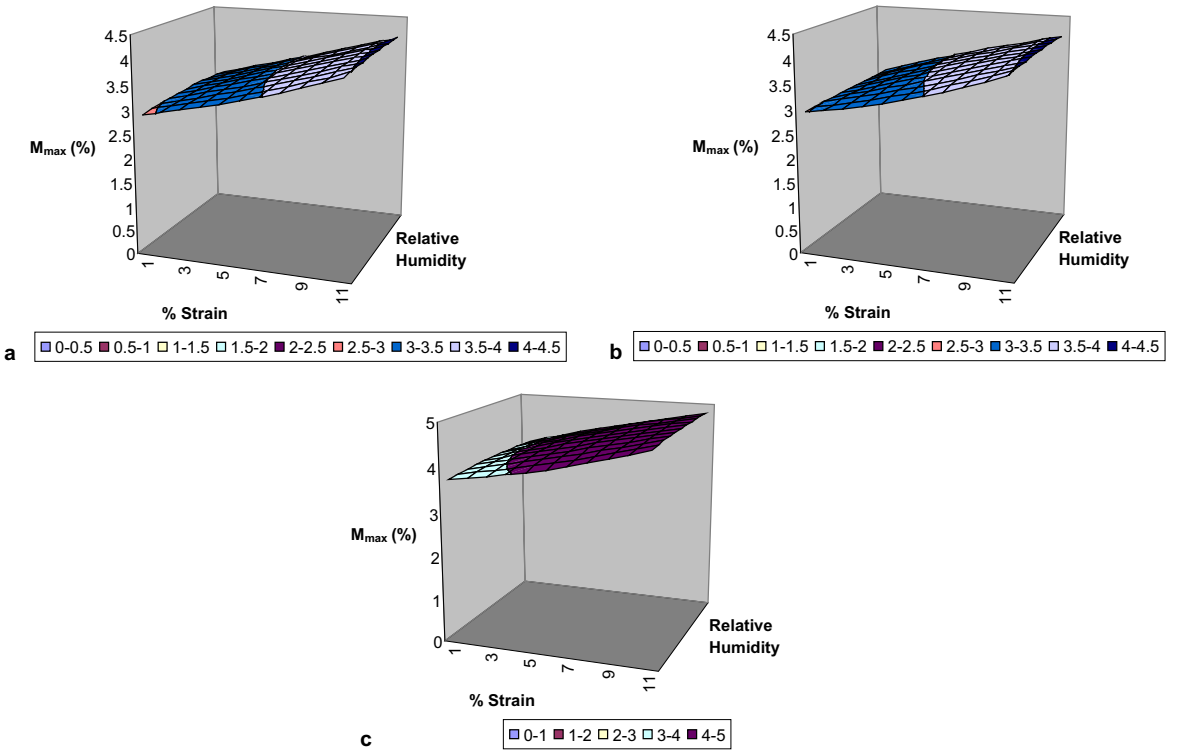

Fig. 16. (a) M_{max} vs strain and RH at 32.2 °C; (b) M_{max} vs strain and relative humidity at 40.5 °C; (c) M_{max} vs strain and RH at 48.9 °C.

4. Conclusions

A strain-assisted diffusion model was developed and experiments were conducted to characterize the material coefficients. The present experiments indicate that the presence of strain in an epoxy based polymer influences the diffusion of water molecules, with significant coupling between applied strain and concentration occurring at elevated humidity levels. It is also evident from the results that there is a consistent increase in diffusivity with strain, whereas the moisture uptake at saturation is affected only beyond 5% strain level, indicating a strain threshold. The mass saturation for 0% and 5% strain level for a given environmental temperature and relative humidity remains approximately constant. While we do not yet have a mechanism-based explanation for this phenomenon, we have used microscopic examination of the specimens to enable us to eliminate damage (microcrack) evolution at elevated strains to be the mechanism responsible for accelerated diffusion. The moisture sorption-desorption data indicates that the moisture diffusion in this material occurs in a concentration-dependent Fickian manner rather than non-Fickian diffusion. If the material exhibited strain gradient dependent non-Fickian behavior where the influence of the strain gradient terms were significant, then the entire set of experiments would have to be repeated with very small strain, perhaps 0.5%, so that the strain gradient effect is negligible and the diffusion coefficients associated with strain gradient would have to be characterized by a numerical iterative procedure.

The coupled strain-assisted diffusion model developed and characterized here will be applied to simulate debond growth in a cohesive layer with moisture diffusion occurring from the crack tip in the presence of applied strain and strain gradients transverse to the bonded interface as depicted in Fig. 1. In order

to define the coupled traction-separation law required for such analyses, characterization of the influence of temperature, humidity, and debond growth rate on adhesive fracture energy is currently underway using the generalized J-integral.

Acknowledgement

This research was funded by the CMS division of the National Science Foundation, Grant Number CMS-0296167.

Appendix A

$$f_1(m_{\max}, \overline{T}, \bar{\varepsilon}_{22}) = 1$$
$$f_2(m_{\max}, \overline{T}, \bar{\varepsilon}_{22}) = m_{\max}$$
$$f_3(m_{\max}, \overline{T}, \bar{\varepsilon}_{22}) = \overline{T}$$
$$f_4(m_{\max}, \overline{T}, \bar{\varepsilon}_{22}) = m_{\max}^2$$
$$f_5(m_{\max}, \overline{T}, \bar{\varepsilon}_{22}) = \overline{T}^2$$
$$f_6(m_{\max}, \overline{T}, \bar{\varepsilon}_{22}) = m_{\max}\overline{T}$$
$$f_7(m_{\max}, \overline{T}, \bar{\varepsilon}_{22}) = m_{\max}\overline{T}^2$$
$$f_8(m_{\max}, \overline{T}, \bar{\varepsilon}_{22}) = m_{\max}^2\overline{T}$$
$$f_9(m_{\max}, \overline{T}, \bar{\varepsilon}_{22}) = m_{\max}^2\overline{T}^2$$
$$f_{10}(m_{\max}, \overline{T}, \bar{\varepsilon}_{22}) = \bar{\varepsilon}_{22}$$
$$f_{11}(m_{\max}, \overline{T}, \bar{\varepsilon}_{22}) = m_{\max}\bar{\varepsilon}_{22}$$
$$f_{12}(m_{\max}, \overline{T}, \bar{\varepsilon}_{22}) = \overline{T}\bar{\varepsilon}_{22}$$
$$f_{13}(m_{\max}, \overline{T}, \bar{\varepsilon}_{22}) = m_{\max}^2\bar{\varepsilon}_{22}$$
$$f_{14}(m_{\max}, \overline{T}, \bar{\varepsilon}_{22}) = \overline{T}^2\bar{\varepsilon}_{22}$$
$$f_{15}(m_{\max}, \overline{T}, \bar{\varepsilon}_{22}) = m_{\max}\overline{T}\bar{\varepsilon}_{22}$$
$$f_{16}(m_{\max}, \overline{T}, \bar{\varepsilon}_{22}) = m_{\max}\overline{T}^2\bar{\varepsilon}_{22}$$
$$f_{17}(m_{\max}, \overline{T}, \bar{\varepsilon}_{22}) = m_{\max}^2\overline{T}\bar{\varepsilon}_{22}$$
$$f_{18}(m_{\max}, \overline{T}, \bar{\varepsilon}_{22}) = m_{\max}^2\overline{T}^2\bar{\varepsilon}_{22}$$
$$f_{19}(m_{\max}, \overline{T}, \bar{\varepsilon}_{22}) = \bar{\varepsilon}_{22}^2$$
$$f_{20}(m_{\max}, \overline{T}, \bar{\varepsilon}_{22}) = m_{\max}\bar{\varepsilon}_{22}^2$$
$$f_{21}(m_{\max}, \overline{T}, \bar{\varepsilon}_{22}) = \overline{T}\bar{\varepsilon}_{22}^2$$
$$f_{22}(m_{\max}, \overline{T}, \bar{\varepsilon}_{22}) = m_{\max}^2\bar{\varepsilon}_{22}^2$$
$$f_{23}(m_{\max}, \overline{T}, \bar{\varepsilon}_{22}) = \overline{T}^2\bar{\varepsilon}_{22}^2$$
$$f_{24}(m_{\max}, \overline{T}, \bar{\varepsilon}_{22}) = m_{\max}\overline{T}\bar{\varepsilon}_{22}^2$$

$$f_{25}(m_{\max}, \overline{T}, \bar{\varepsilon}_{22}) = m_{\max}\overline{T}^2\bar{\varepsilon}_{22}^2$$
$$f_{26}(m_{\max}, \overline{T}, \bar{\varepsilon}_{22}) = m_{\max}^2\overline{T}\bar{\varepsilon}_{22}^2$$
$$f_{27}(m_{\max}, \overline{T}, \bar{\varepsilon}_{22}) = m_{\max}^2\overline{T}^2\bar{\varepsilon}_{22}^2$$

Appendix B

$$f_1(RH, \overline{T}, \varepsilon_b) = 1$$
$$f_2(RH, \overline{T}, \varepsilon_b) = RH$$
$$f_3(RH, \overline{T}, \varepsilon_b) = \overline{T}$$
$$f_4(RH, \overline{T}, \varepsilon_b) = RH^2$$
$$f_5(RH, \overline{T}, \varepsilon_b) = \overline{T}^2$$
$$f_6(RH, \overline{T}, \varepsilon_b) = RH\overline{T}$$
$$f_7(RH, \overline{T}, \varepsilon_b) = RH\overline{T}^2$$
$$f_8(RH, \overline{T}, \varepsilon_b) = RH^2\overline{T}$$
$$f_9(RH, \overline{T}, \varepsilon_b) = RH^2\overline{T}^2$$
$$f_{10}(RH, \overline{T}, \varepsilon_b) = \varepsilon_b$$
$$f_{11}(RH, \overline{T}, \varepsilon_b) = RH\varepsilon_b$$
$$f_{12}(RH, \overline{T}, \varepsilon_b) = \overline{T}\varepsilon_b$$
$$f_{13}(RH, \overline{T}, \varepsilon_b) = RH^2\varepsilon_b$$
$$f_{14}(RH, \overline{T}, \varepsilon_b) = \overline{T}^2\varepsilon_b$$
$$f_{15}(RH, \overline{T}, \varepsilon_b) = RH\overline{T}\varepsilon_b$$
$$f_{16}(RH, \overline{T}, \varepsilon_b) = RH\overline{T}^2\varepsilon_b$$
$$f_{17}(RH, \overline{T}, \varepsilon_b) = RH^2\overline{T}\varepsilon_b$$
$$f_{18}(RH, \overline{T}, \varepsilon_b) = RH^2\overline{T}^2\varepsilon_b$$
$$f_{19}(RH, \overline{T}, \varepsilon_b) = \varepsilon_b^2$$
$$f_{20}(RH, \overline{T}, \varepsilon_b) = RH\varepsilon_b^2$$
$$f_{21}(RH, \overline{T}, \varepsilon_b) = \overline{T}\varepsilon_b^2$$
$$f_{22}(RH, \overline{T}, \varepsilon_b) = RH^2\varepsilon_b^2$$
$$f_{23}(RH, \overline{T}, \varepsilon_b) = \overline{T}^2\varepsilon_b^2$$
$$f_{24}(RH, \overline{T}, \varepsilon_b) = RH\overline{T}\varepsilon_b^2$$
$$f_{25}(RH, \overline{T}, \varepsilon_b) = RH\overline{T}^2\varepsilon_b^2$$
$$f_{26}(RH, \overline{T}, \varepsilon_b) = RH^2\overline{T}\varepsilon_b^2$$
$$f_{27}(RH, \overline{T}, \varepsilon_b) = RH^2\overline{T}^2\varepsilon_b^2$$

References

Crank, J., 1975. The Mathematics of Diffusion, second ed. Oxford University Press.

Fahmy, A.A., Hurt, J.C., 1980. Stress dependence of water diffusion in epoxy resin. Polymer Composites 1, 77–80.

Gere, J., Timoshenko, S., 1984. Mechanics of Materials. PWS-Kent Publishing Company.

Roy, S., 1999. Modeling of Anomalous Diffusion in Polymer Composites: A Finite Element Approach. Journal of Composite Materials 33 (14), 1318–1343.

Roy, S., Shiue, F.W., 2003. A Coupled Hygrothermal Cohesive-Layer Constitutive Model for Simulating Debond Growth. Polymer and Polymer Composites 11 (8), 633–647.

Roy, S., Lefebvre, D.R., Dillard, D.A., Reddy, J.N., 1989. A Model for the Diffusion of Moisture in Adhesive Joints. Part III: Numerical Simulations. Journal of Adhesion 27, 41–62.

Roy, S., Xu, W., Park, S.J., Liechti, K.M., 2000. Anomalous Moisture Diffusion in Viscoelastic Polymers: Modeling and Testing. Journal of Applied Mechanics 67 (June), 391–396.

Roy, S., Xu, W., Patel, S., Case, S., 2001. Modeling of Moisture Diffusion in the Presence of Bi-axial Damage in Polymer Matrix Composite Laminates. International Journal of Solids and Structures 38 (42–43), 7627–7641.

Sancaktar, E., Baechtle, D., 1993. The Effect of Stress Whitening on Moisture Diffusion in Thermosetting Polymers. J. Adhesion 42, 65–85.

Tsai, C., Cheng, M., Hwang, S., Tsai, Y., 2004. Characterizing the Hygric Behavior of Composites by Suspending Method. Journal of Composite Materials 38 (9).

Weitsman, Y., 1987. Stress assisted diffusion in elastic and viscoelastic materials. Journal of Mechanics and Physics of Solids 35, 73–93.

Weitsman, Y., 1991. Moisture in Composites: Sorption and Damage. Fatigue of Composite Materials, 385–429.

Wong, T., Broutman, L., 1985a. Moisture Diffusion in Epoxy Resins Part I: Non-Fickian Sorption Processes. Polymer Eng. Sci. 25 (9), 521–528.

Wong, T., Broutman, L., 1985b. Water in Epoxy Resins Part II: Diffusion Mechanisms. Polymer Eng. & Sci. 25 (9), 529–534.